

Spectroscopic and Structural Characterizations of Novel Water-Soluble Tetraperoxo and Diperoxo[polyaminocarboxylato bis(*N*-oxido)]tantalate(V) ComplexesDaisy Bayot,[†] Bernard Tinant,[‡] and Michel Devillers^{*†}

Unité de Chimie des Matériaux Inorganiques et Organiques, Université Catholique de Louvain, Place Louis Pasteur 1, B-1348 Louvain-la-Neuve, Belgium, and Unité de Chimie Structurale et des Mécanismes Réactionnels, Université Catholique de Louvain, Place Louis Pasteur 1, B-1348 Louvain-la-Neuve, Belgium

Received March 18, 2004

New water-soluble homoleptic peroxo complexes and heteroleptic peroxo-polyaminocarboxylato (PAC) complexes of tantalum(V) have been prepared. In the case of the peroxo-PAC complexes, the synthesis in the presence of excess H₂O₂ leads to the oxidation of the nitrogen atoms of the ligand into *N*-oxides. The compounds correspond to the general formula (gu)₃[Ta(O₂)₂(LO₂)]·*x*H₂O (gu = guanidinium, L = edta or pdta) in which H₄LO₂ refers to the bis(*N*-oxide) derivative of the PAC ligand. The Ta^V complexes have been characterized on the basis of elemental and thermal analysis and by IR and ¹³C and ¹⁵N NMR spectroscopy. These last two spectroscopic methods have been used to suggest the coordination mode of the PAC ligand in the complexes. ESI mass spectrometry measurements have also been carried out for the peroxo-PAC compounds. The crystal structures of the homoleptic tetraperoxo-tantalate, (gu)₃[Ta(O₂)₄] (**1**), and the heteroleptic complex, (gu)₃[Ta(O₂)₂(edtaO₂)]·2.32H₂O·0.68H₂O₂ (**2b**), have been determined, showing, for both cases, an 8-fold-coordinated Ta atom surrounded either by four bidentate peroxides or by two peroxides and one tetradentate edtaO₂ ligand.

Introduction

In the past decade, the peroxo species of transition metals (i.e., Mo, W, V, and Nb) have attracted considerable attention because many of them are efficient stoichiometric or catalytic oxidants for organic substrates.^{1–4} Moreover, for some of these peroxo compounds, a further interest results from the important role they play in biological systems. For example, peroxo-vanadium(V) complexes have been found to have antitumor and insulin mimetic activities, while others have been studied as functional models for the vanadium haloperoxidase enzymes.^{5,6}

Because such peroxo-type coordination compounds are usually soluble in water, they are also of great interest as the molecular precursors for the preparation of oxide materials, more specifically, multimetallic oxides involving transition metals for which the availability of well-defined water-soluble complexes is very limited.

Within the framework of oxide preparation, we already reported the use of peroxo-transition-metal complexes for preparing silica-dispersed Nb–Mo-containing catalysts by combining analogous water-soluble Nb^V and Mo^{VI} molecular precursors.⁷ With respect to Ta^V, its aqueous chemistry is restricted to very few compounds with peroxo ligands, with some of them being poorly defined in the literature from a composition and molecular structure point of view. These complexes correspond either to homoleptic tetraperoxo-tantalates of the general formula (A^I)₃[Ta(O₂)₄] (A^I = K⁺ or NH₄⁺)^{8,9} or to heteroleptic peroxo-carboxylato compounds, such as K₃[Ta(O₂)₃(L)]·*x*H₂O, with L = tartrate, citrate,

* Author to whom correspondence should be addressed. Tel: + 32-10/472827. Fax: + 32-10/472330. E-mail: devillers@chim.ucl.ac.be.

[†] Unité de Chimie des Matériaux Inorganiques et Organiques.

[‡] Unité de Chimie Structurale et des Mécanismes Réactionnels.

- (1) Passoni, L. C.; Siddiqui, M. R. H.; Steiner, A.; Kozhevnikov, I. V. *J. Mol. Catal. A: Chem.* **2000**, *153*, 103–108.
- (2) Bonchio, M.; Bortolini, O.; Conte, V.; Primon, S. *J. Chem. Soc., Perkin Trans. 2* **2001**, 763–765.
- (3) Conte, V.; DiFuria, F.; Moro, S. *J. Phys. Org. Chem.* **1996**, *9*, 329–336.
- (4) Campestrini, S.; DiFuria, F. *Tetrahedron* **1994**, *50*, 5119–5130.
- (5) Crans, D. C.; Smee, J. J.; Gaidamauskas, E.; Yang, L. Q. *Chem. Rev.* **2004**, *104*, 849–902.

(6) Thompson, K. H.; McNeill, J. H.; Orvig, C. *Chem. Rev.* **1999**, *99*, 2561–2571.

(7) Bayot, D.; Tinant, B.; Devillers, M. *Catal. Today* **2003**, *78*, 439–447.

glycolate, dipicolinate, or *o*-phenanthroline, and $K_3[Ta(O_2)_2(C_2O_4)_2] \cdot H_2O$.^{10,11} Among these compounds, the only crystal structure reported is that of the potassium salt $K_3[Ta(O_2)_4]$,⁹ and the literature reports only one Ta complex with a polyaminocarboxylate (PAC) ligand that is wrongly described by Vuletic et al. as the ammonium-peroxo-edta compound, $(NH_4)_3[Ta(O_2)_3H_2(edta)]$.¹² We also recently reported the preparation and characterization of peroxo-polyaminocarboxylato Nb^V complexes in which the synthesis in the presence of excess H₂O₂ was shown to cause in situ oxidation of the nitrogen atoms of the PAC ligand into *N*-oxides.¹³ Because tantalum also belongs to group 5, we expected Ta^V would display a similar behavior toward such ligands, creating new perspectives for an extended aqueous chemistry of this rarely used element.

Within the context of Ta-containing oxide materials preparation, the present work describes new water-soluble peroxo-polyaminocarboxylato Ta^V compounds corresponding to the general formula $(A^1)_3[Ta(O_2)_2(LO_2)] \cdot xH_2O$, with $A^1 =$ guanidinium (gu, $CN_3H_6^+$), in which H_4LO_2 refers to the bis(*N*-oxide) derivative of the PAC ligand (L). Two different ligands have been selected: ethylenediaminetetraacetic acid (H_4edta) and propylenediaminetetraacetic acid (H_4pdta).

Experimental Section

General. All of the manipulations were carried out in aqueous solution. Ethylenediaminetetraacetic acid, H_4edta (Fluka), propylenediaminetetraacetic acid, H_4pdta (Fluka), and guanidinium carbonate, $(gu)_2CO_3$ (Aldrich), were commercial products used as they were received. Hydrogen peroxide, H₂O₂ (35 wt %, Acros), aqueous ammonia (25 wt %), acetone, and ethanol were used without purification. Tantalum pentachloride, TaCl₅, was purchased from Alfa and kept in a glovebox under an inert atmosphere until it was used. Elemental analyses (C, H, and N) were carried out at the University College of London. IR spectra in the 4000–400 cm⁻¹ range were recorded on a FTS-135 Bio-RAD spectrometer, using KBr pellets containing ca. 1 wt % of the powder. Thermogravimetric analyses (TGA) were performed in air at a heating rate of 10 °C/min using a Mettler Toledo TGA/SDTA851^e analyzer. ¹³C and ¹⁵N NMR spectra were measured in D₂O at 125 and 50 MHz, respectively, on a Bruker Avance 500 MHz spectrometer equipped with a broad-band inverse probe. ¹⁵N NMR spectra were recorded using the HMBC pulse sequence with a mixing time of 100 ms. Chemical shifts are expressed in parts per million and are referenced from TMS for ¹³C (0 ppm) or nitromethane for ¹⁵N (375 ppm). The nano-electrospray ionization mass spectrometry (NESI-MS) measurements were obtained on a Finnigan MAT LCQ instrument. The samples were introduced by the injection of the complex (0.001 mol·L⁻¹) and dissolved in CH₃OH/H₂O (1:1, v/v).

The homoleptic guanidinium tetraperoxotantalate complex, $(gu)_3[Ta(O_2)_4]$, was synthesized in the same manner that was used for the similar niobium derivative.¹³ The heteroleptic peroxo-polyami-

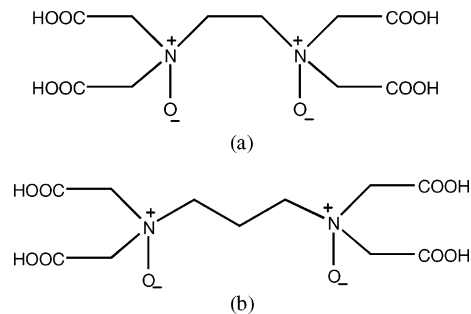


Figure 1. Chemical structures of (a) H_4edtaO_2 and (b) H_4pdtaO_2 .

nocarboxylato Ta^V complexes were prepared by substituting the peroxo groups with a PAC ligand in the tetraperoxotantalate anion $[Ta(O_2)_4]^{3-}$ in an aqueous medium. These syntheses were carried out in the presence of excess hydrogen peroxide which led to the in situ formation of the *N*-oxide derivative of the commercial PAC ligand (Method A). These bis(*N*-oxide) PAC ligands, $H_4edtaO_2 \cdot 1/2H_2O$ and $H_4pdtaO_2 \cdot H_2O$, were also synthesized separately following the procedure of Beltran Porter et al.¹⁴ The preparation and characterization details are described elsewhere.¹³ Figure 1 displays the chemical structures of both of the *N*-oxide ligands that were used. The peroxo-PAC Ta^V complexes were also prepared from these preisolated modified ligands (Method B). Both synthetic pathways were shown to lead to the same compounds.

Synthesis of $(gu)_3[Ta(O_2)_4]$ (1). TaCl₅ (5 g, 13.95 mmol) was hydrolyzed in 50 mL of distilled water and 4 mL of ammonia (25 wt % solution). The resulting cloudy solution was stirred for 1 h at room temperature. The white solid obtained was filtered off and washed several times with warm water until no Cl⁻ ions were detected in the filtrate (Ag⁺ test). A slurry of this solid in 50 mL of distilled water was treated with 20 mL of H₂O₂ (35 wt % solution) and $(gu)_2CO_3$ (3.77 g, 20.9 mmol) and stirred for a few hours. When the solid was totally dissolved, the addition of 100 mL of acetone produced a white crystalline precipitate, which was filtered off, washed with acetone, and air-dried. The yield was 94%. Anal. Calcd for C₃N₉H₁₈TaO₈: C, 7.42; H, 3.10; N, 25.96. Found: C, 7.62; H, 3.64; N, 25.75.

The slow evaporation at room temperature of an aqueous concentrated solution yielded small white monocrystals of **1**, which were suitable for structure determination by single-crystal X-ray diffraction.

Synthesis of $(gu)_3[Ta(O_2)_2(edtaO_2)] \cdot 2H_2O$ (2a). **Method A.** $(gu)_3[Ta(O_2)_4]$, **1** (1.03 g, 2.11 mmol), was dissolved in 50 mL of distilled water and 10 mL of H₂O₂ (35 wt % solution). H_4edta (0.616 g, 2.11 mmol) was added gradually. The resulting clear solution was then gently heated for 10 min ($T = 60$ °C), and the solvent was evaporated under reduced pressure to a final volume of 20 mL. The addition of 150 mL of ethanol precipitated a white crystalline solid which was filtered off, washed with ethanol, and air-dried.

Method B. $(gu)_3[Ta(O_2)_4]$, **1** (1.03 g, 2.11 mmol), was dissolved in 50 mL of distilled water, and $H_4edtaO_2 \cdot 1/2H_2O$ (0.703 g, 2.11 mmol) was added gradually. The following steps of the synthesis were the same as those for method A. The yield was 85%. Anal. Calcd for C₁₃N₁₁H₃₄TaO₁₆: C, 19.97; H, 4.35; N, 19.71. Found: C, 20.43; H, 4.28; N, 19.17.

The slow evaporation at room temperature of an aqueous concentrated solution yielded white monocrystals that were suitable for structure determination by single-crystal X-ray diffraction and

(8) Selezneva, K. I.; Nisel'son, L. A. *Russ. J. Inorg. Chem.* **1968**, *13*, 45–47.

(9) Wehrum, G.; Hoppe, R. Z. *Anorg. Allg. Chem.* **1993**, *619*, 1315–1320.

(10) Dengel, A. C.; Griffith, W. P. *Polyhedron* **1989**, *8*, 1371–1377.

(11) Djordjevic, C.; Vuletic, N. *Inorg. Chem.* **1968**, *7*, 1864–1868.

(12) Vuletic, N.; Prcic, E. Z. *Anorg. Allg. Chem.* **1979**, *450*, 67–69.

(13) Bayot, D.; Tinant, B.; Mathieu, B.; Declercq, J. P.; Devillers, M. *Eur. J. Inorg. Chem.* **2003**, 737–743.

(14) Beltran Porter, B.; de Haro Rodriguez, M.; Penalver Conesa, P. *Afinidad* **1976**, *33*, 489–495.

Table 1. Crystal Data and Structure Refinement Parameters for **1** and **2b**

	1	2b
formula	C ₃ H ₁₈ N ₉ TaO ₈	C ₁₃ H ₃₀ N ₁₁ TaO ₁₄ · 2.32H ₂ O·0.68H ₂ O ₂
fw	489.21	810.32
<i>T</i> (K)	293 ± 2	110 ± 2
crystal system	monoclinic	triclinic
space group	<i>Pn</i>	<i>P1</i>
unit cell dimensions		
<i>a</i> (Å)	8.572(3)	11.091(3)
<i>b</i> (Å)	10.327(5)	11.436(3)
<i>c</i> (Å)	8.874(3)	11.762(3)
α (deg)	90	99.79(2)
β (deg)	103.08(2)	102.85(2)
γ (deg)	90	93.66(2)
<i>V</i> (Å ³)	765.2(5)	1425.3(6)
<i>Z</i>	2	2
<i>D</i> _{calcd} (g·cm ⁻³)	2.12	1.89
μ (mm ⁻¹)	7.236	3.956
<i>F</i> (000)	462	796
crystal size (mm)	0.32 × 0.28 × 0.24	0.30 × 0.26 × 0.26
θ range (deg)	2.98–27.48	2.76–26.40
<i>hkl</i> ranges	0 ≤ <i>h</i> ≤ 10 0 ≤ <i>k</i> ≤ 13 −11 ≤ <i>l</i> ≤ 11	0 ≤ <i>h</i> ≤ 13 −14 ≤ <i>k</i> ≤ 14 −14 ≤ <i>l</i> ≤ 14
reflections collected/unique	9258/1745	12664/5473
<i>R</i> _{int}	0.068	0.038
data/restraints/parameters	1745/2/192	5473/2/401
<i>R</i> ₁ , <i>wR</i> ₂ [<i>I</i> > 2σ(<i>I</i>)] ^a	0.035, 0.102 [1700]	0.038, 0.100 [5426]
<i>R</i> ₁ , <i>wR</i> ₂ (all data)	0.035, 0.103	0.039, 0.101
GOF on <i>F</i> ²	1.154	1.139
largest diff. peak (eÅ ⁻³)	3.139/−1.600	2.556/−2.240

$$^a R_1 = \sum ||F_0| - |F_c|| / \sum |F_0|, wR_2 = [(\sum (F_0^2 - F_c^2)^2) / \sum (wF_0^2)]^{1/2}.$$

corresponded to the stoichiometry of (gu)₃[Ta(O₂)₂(edtaO₂)]·2.32H₂O·0.68H₂O₂ (**2b**).

Synthesis of (gu)₃[Ta(O₂)₂(pdtaO₂)]·H₂O (3**).** This compound was prepared in the same manner as complex **2a**. The synthesis was carried out from compound **1** (1 g, 2.05 mmol) by replacing H₄edta with H₄pdta (0.626 g, 2.05 mmol) in Method A and by replacing H₄edtaO₂·½H₂O with H₄pdtaO₂·H₂O (0.73 g, 2.05 mmol) in Method B. The yield was 87%. Anal. Calcd for C₁₄N₁₁H₃₄TaO₁₅: C, 21.62; H, 4.37; N, 19.81. Found: C, 21.59; H, 4.33; N, 19.09.

No suitable monocrystal of compound **3** could be obtained by applying the same method as for **1** and **2**.

Caution! *Tetraperoxo and peroxo-PAC tantalum complexes are potentially explosive when heated above 100 °C. They should preferably be handled at room temperature.*

X-ray Crystallography. The X-ray intensity data were measured at room temperature for **1**. The data were collected at 110 K for **2b** with a MAR345 image plate using Mo Kα (λ = 0.71069 Å) radiation. The selected crystal was mounted in inert oil and transferred to the cold gas stream for flash cooling. The crystal data and data collection parameters are summarized in Table 1. The unit cell parameters were refined using all of the collected spots after the integration process. The data were not corrected for absorption, but the data collection mode (80 images, ΔΦ 3°, 9258 reflections measured for 1745 unique reflections) partially takes the absorption phenomena into account.

Both structures were solved by the Patterson method, followed by the Fourier difference synthesis, and refined by the full-matrix least-squares on *F*² using SHELXL-97.¹⁵ The structure of **1** is isomorphous with that of (gu)₃[Nb(O₂)₄].⁷ There was a choice

between the acentric space group *Pn* and the centric groups *P2/n* and *P21/n*. The statistics on the intensities indicated noncentrosymmetry. Refinements in the two possible centric space groups have been tested, but they did not converge to satisfying *R* values. All of the non-hydrogen atoms were refined anisotropically. The hydrogen atoms were calculated with AFIX and included in the refinement with a common isotropic temperature factor. In the structure of **2b**, the H atoms of the water and hydrogen peroxide molecules are not localized. At the end of the refinement, the temperature factors of the O201 and O301 atoms of the hydrogen peroxide molecules were abnormally large, especially compared to their bonded atoms, O200 and O300. Because sharing of the same sites for H₂O and H₂O₂ is common, we have refined a site-occupation factor for each O201 and O301. At the end of the refinement, these site occupation factors converge to 0.29 and 0.39, respectively. The triclinic unit cell of **2b** is similar to that reported for the corresponding Nb complex,¹³ but with a *c* parameter approximately 2-fold shorter. In the structure reported here, there are only one anion, three guanidinium cations, and three sites shared between water and hydrogen peroxide molecules in the asymmetric unit, compared with two anions, six guanidinium cations, six water molecules, and two H₂O₂ molecules for the Nb derivative.¹³

The details of the refinement and the final *R* indices are presented in Table 1. In each structure, the largest peak in the final Fourier difference synthesis is located near a Ta atom.

Results and Discussion

General Comments on Peroxo Compounds of Group 5 Elements. The obtained peroxo complexes of tantalum(V) are very similar to those of niobium(V) reported recently.¹³ Both elements display quasi-identical chemical behaviors. The preparation procedures applied for niobium could be transposed to tantalum. With respect to vanadium, also belonging to group 5, its “peroxo chemistry” is very different from that of Nb or Ta. Unlike Nb and Ta, vanadium has a strong tendency to form oxoperoxo species. The majority of peroxo-type complexes of V^V described in the literature displays one or more vanadyl bonds.^{5,6} In addition, bridging vanadium-peroxo derivatives form very easily. In this respect, vanadium more resembles molybdenum or tungsten. The structure of the vanadium complexes (number of peroxo, vanadyl groups, and auxiliary organic ligands) is dictated by several parameters such as pH and H₂O₂ concentration, while for Nb and Ta, this is not the case. For example, although the tetraperoxo-niobate and -tantalate compounds are stable in solution, K₃[V(O₂)₄] is stable at pH > 13.5 only and usually transforms into species such as [VO(O₂)₃]³⁻ or [V₂O₃(O₂)₄]⁴⁻, depending on the pH and H₂O₂ concentration.¹⁶ Moreover, while vanadium atoms are generally 6- or 7-fold-coordinated (rarely 8-fold), the coordination number around Nb and Ta in the peroxo compounds is always eight, as has been reported.

IR Spectroscopy. Table 2 lists (for compounds **1–3**) the infrared bands which can clearly be assigned to the typical vibration modes of the coordinated side-bonded peroxo ligands, the O–O stretching, ν(O–O) in the range 800–850 cm⁻¹, and the asymmetric metal-peroxo stretching, ν_{as-}

(15) Sheldrick, G. M. *Program for crystal structure refinement*; University of Göttingen: Göttingen, Germany, 1997.

(16) Campbell, N. J.; Dengel, A. C.; Griffith, W. P. *Polyhedron* **1989**, *8*, 1379–1386.

Table 2. Infrared Data (in cm^{-1}) for Compounds **1–3**^a

	$\nu(\text{O}-\text{O})$	$\nu_{\text{as}}[\text{Ta}(\text{O}_2)]$	$\nu_{\text{as}}(\text{COO})$	$\nu_{\text{s}}(\text{COO})$	$\nu(\text{N}-\text{O})$
1	817s 809s	551m			
2a	858m 843m	539m	1661s 1624s	1377s 1392s	907m
3	861m 846m	553m	1625s 1656s	1380s	899m

^a s = strong, m = medium, w = weak.

Table 3. ¹³C and ¹⁵N NMR Chemical Shifts (δ , ppm) for Compounds **2a** and **3** and Commercial or Oxidized PAC Ligands

	¹³ C NMR line (ppm) ^a	¹⁵ N NMR line (ppm) ^a	ref
2a	60.6, 67.8, 74.1, 171.4, 172	66.5, 120.8	this work
3	21.9, 57.7, 69.1, 70.7, 160.5, 173.6	68.2, 123.6	this work
H ₄ edtaO ₂ /NaOD ^b	59.7, 67.5, 170.6	114.9	13
H ₄ pdtAO ₂ /NaOD ^b	19.1, 64.9, 66.6, 171.4	123.6	13
H ₄ edta/NaOD ^b	50.9, 57.5, 176.9	38.5	13
H ₄ pdtA/NaOD ^b	23.0, 53.2, 58.9, 179.3	53.1	13

^a In D₂O. ^b H₄L and H₄LO₂ compounds are not soluble in D₂O at room temperature and were solubilized by adding an excess of NaOD (pH \geq 4).

[Ta(O₂)] arising near 550 cm^{-1} . In the case of **2a** and **3**, some representative vibrational modes of the coordinated PAC ligands and the bands arising from the *N*-oxide groups are also listed.

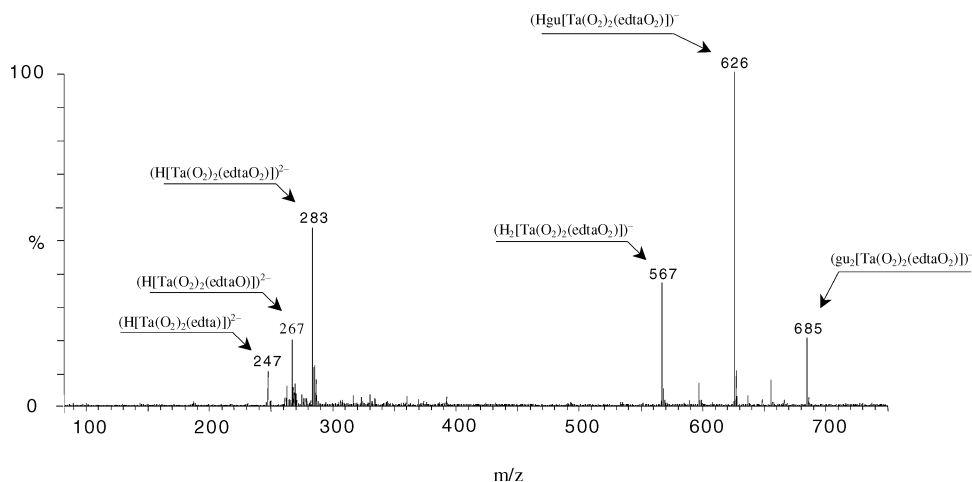
The IR spectrum of the tetraperoxotantalate **1** displays two $\nu(\text{O}-\text{O})$ bands of high intensity at 809 and 817 cm^{-1} and is very similar to that obtained for the corresponding niobium derivative, (gu)₃[Nb(O₂)₄].⁷ The IR spectra of **2a** and **3** show two $\nu(\text{O}-\text{O})$ bands of medium intensity in the range 850–860 cm^{-1} . Next to this, the asymmetric stretching frequency of the carboxylato groups complexed to tantalum appears (in **2a** and **3**) as a strong broad band near 1650 cm^{-1} . Coordination of the tantalum atom by these carboxylato groups is evident by the broadening of the $\nu_{\text{as}}(\text{COO})$ band and by its significant shift from a value of ca. 1700 cm^{-1} in the free PAC acid to ca. 1650 cm^{-1} in the complex. Finally, oxidation of the nitrogen atoms of the PAC ligand during the syntheses (excess H₂O₂ medium) is evident by the

presence (in the IR spectra of **2** and **3**) of the $\nu(\text{N}-\text{O})$ band near 900 cm^{-1} . In the corresponding bis(*N*-oxide) derivative of the free ligands, H₄edtaO₂· $\frac{1}{2}$ H₂O and H₄pdtAO₂·H₂O, this band appears at 890 and 909 cm^{-1} , respectively.¹³

NMR Spectroscopy. Table 3 lists the ¹³C and ¹⁵N resonance lines occurring in compounds **2a** and **3** and, for comparison, the values reported for the commercial and oxidized PAC ligands.¹³

Similar to the infrared spectroscopy, the ¹⁵N NMR analyses of the prepared peroxo-PAC complexes reveal the oxidation of the nitrogen atoms in the ligand. The ¹⁵N NMR spectrum of **2a** displays one line at $\delta = 66.5$, arising from the carbon atom in the guanidinium counterions. It also shows another line at $\delta = 120.8$, assigned to the two identical nitrogen atoms in the ligand. This particularly high ¹⁵N chemical shift displays the formation of *N*-oxide groups when compared with the values obtained for the H₄edta and H₄edtaO₂ species, $\delta = 38.5$ (ternary nitrogen) and 114.9 (quaternary oxidized nitrogen), respectively. In the ¹⁵N NMR analysis of **3**, the assignment of the two signals observed at $\delta = 68.2$ and 123.6 is the same as that of **2a**. In the free H₄pdtA and H₄pdtAO₂, the lines arising from the two N atoms inside the ligand occur at $\delta = 53.1$ and 123.6, respectively.

Information on the coordination mode of the bis(*N*-oxide) ligand is provided by the ¹³C NMR analysis. The ¹³C NMR spectrum of the [Ta(O₂)₂(edtaO₂)]³⁻ anion shows three lines at $\delta = 60.6$, 67.8, and 74.1, arising from the CH₂ groups of the edta ligand. These carbon atoms are clearly influenced by the complexation process. Although all four CH₂ moieties from the acetate groups occur as one single peak in the free ligand ($\delta = 50.9$), they undergo a significant variation in chemical shift and are differentiated in the complex ($\delta = 60.6$ and 67.8). Moreover, the CH₂ groups of the *N*-bound ethylene moiety are not differentiated (they arise as one single line as in H₄edta), but they are shifted from $\delta = 57.5$ in the free ligand to $\delta = 74.1$ in the complex. A shift is also observed for these carbon atoms in the free bis(*N*-oxide) edta ligand ($\delta = 67.5$). This result shows, once more, the presence of the *N*-O groups in the coordinated ligand. The resonance signal corresponding to the quaternary carbons from the carboxylato groups in the complex is differentiated (two

**Figure 2.** Negative ion mass spectrum of compound **2a** in CH₃OH/H₂O.

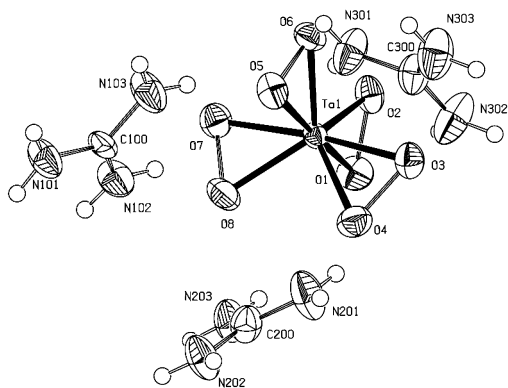


Figure 3. ORTEP plot of $(\text{gu})_3[\text{Ta}(\text{O}_2)_4]$ (50% probability).²¹

resonance signals) in comparison with that of the free ligand (one single line). The presence of two ^{13}C lines at $\delta = 171.4$ and 172.0 implies that two carboxylato groups are coordinated to Ta, and the two other groups remain free. The complete analysis of the ^{13}C NMR spectrum of **2a** allows us to determine the coordination mode of the ligand to the tantalum atom: the bis(*N*-oxide)edta is tetradentate, with the four binding atoms being oxygens from two carboxylates (each placed on a different N atom) and two *N*-oxide groups. A similar analysis based on the ^{13}C NMR lines observed for **3** leads to the same conclusion about the coordination mode of the bis(*N*-oxide)pdta ligand. Some additional peaks of weak intensity are also observed at $\delta = 19.3, 65.1, 66.8,$ and 171.7 and arise from free pdtaO₂ ligands. This indicates that the $[\text{Ta}(\text{O}_2)_2(\text{pdtaO}_2)]^{3-}$ species is present in solution but decomposes partially with the release of the free ligand. This phenomenon was not observed in the case of the edta derivative, **2a**.

Mass Spectrometry. The negative ion NESI mass spectrum of compound **2a** (illustrated in Figure 2) shows the major peaks at m/z 567, 626, and 685, which can be assigned to the parent ion combined with H^+ and/or the counterion guanidinium (gu^+) and corresponding to the singly charged species $(\text{H}_2[\text{Ta}(\text{O}_2)_2(\text{edtaO}_2)])^-$, $(\text{H}(\text{gu})[\text{Ta}(\text{O}_2)_2(\text{edtaO}_2)])^-$, and $(\text{gu})_2[\text{Ta}(\text{O}_2)_2(\text{edtaO}_2)]^-$, respectively. Moreover, the parent ion combined with one H^+ ion, $(\text{H}[\text{Ta}(\text{O}_2)_2(\text{edtaO}_2)])^{2-}$, is observed at m/z 283 along with the ions derived from the successive losses of both oxygen atoms from the *N*-oxide groups in the edtaO₂ ligand (m/z 267 and 247). The mass spectrum obtained for compound **3** displays peaks at m/z 640 and 699, which can be assigned to the singly charged species $(\text{H}(\text{gu})[\text{Ta}(\text{O}_2)_2(\text{pdtaO}_2)])^-$ and $(\text{gu})_2[\text{Ta}(\text{O}_2)_2(\text{pdtaO}_2)]^-$, respectively, similar to those of the edtaO₂ complex, **2a**. Moreover, the parent ion combined with two H^+ ions, $(\text{H}_2[\text{Ta}(\text{O}_2)_2(\text{edtaO}_2)])^-$, is observed at m/z 581, and the ions derived from the successive losses of oxygen atoms from both *N*-oxide groups in the pdtaO₂ ligand (m/z 565 and 549) are also observed. This phenomenon, also observed for compound **2**, provides further evidence of the in situ *N*-oxidation of the ligand when the syntheses are carried out with the commercial H_4edta and H_4pdta .

X-ray Crystal Structures. The asymmetric unit of **1** consists of one $[\text{Ta}(\text{O}_2)_4]^{3-}$ anion and three guanidinium cations. No solvent molecule was found. For **2b**, the structure

Table 4. Selected Bond Lengths and Deviations from Mean Peroxo Plane (Å) for **1** and **2b**

		deviation from mean plane through four O(peroxo)		
1				
Ta–O(peroxo)	2.005(8)	1.961(7)	O1	0.0167
	2.053(7)	2.019(7)	O2	−0.0244
	2.052(7)	1.997(7)	O5	−0.0165
	2.030(7)	2.015(8)	O6	0.0241
	1.492(8)		O3	−0.0036
O–O(peroxo)	1.511(8)		O4	0.0053
	1.509(6)		O7	0.0036
	1.489(8)		O8	−0.0054
	2b			
	Ta–O(carboxylate)	2.130(4)		O23
2.136(4)			O24	−0.0026
Ta–O(peroxo)			O25	−0.0026
			O26	0.0026
			O10	−2.6653
			O18	−2.7739
			O1	−1.6854
Ta–O(<i>N</i> -oxide)	2.084(4)		O22	−1.7675
	2.099(4)		Ta	−1.1728
Ta–O(peroxo)	1.969(4)			
	1.995(4)			
	1.997(4)			
	2.007(4)			
O–O(peroxo)	1.507(6)			
	1.482(6)			
N–O(<i>N</i> -oxide)	1.393(6)			
	1.392(6)			

consists of one $[\text{Ta}(\text{O}_2)_2(\text{edtaO}_2)]^{3-}$ anion, three guanidiniums, and three sites shared between water and hydrogen peroxide molecules.

In crystal **1**, as observed for $\text{K}_3[\text{Ta}(\text{O}_2)_4]$ ⁹ or for the niobium derivative $(\text{gu})_3[\text{Nb}(\text{O}_2)_4]$,⁷ which is isomorphous, Ta is 8-fold-coordinated. The four peroxide groups are bidentate (as illustrated in Figure 3), and the coordination polyhedron is a dodecahedron. The four oxygen atoms, O1, O2, O5, and O6, are actually coplanar, within experimental error, and the O3, O4, O7, and O8 atoms are, as well. As indicated in Table 4, the maximum deviation from the best mean plane through these two groups of O atoms is <0.03 and 0.006 Å, respectively. Moreover, the experimental angle between these two planes is $89(1)^\circ$. All the Ta–O distances

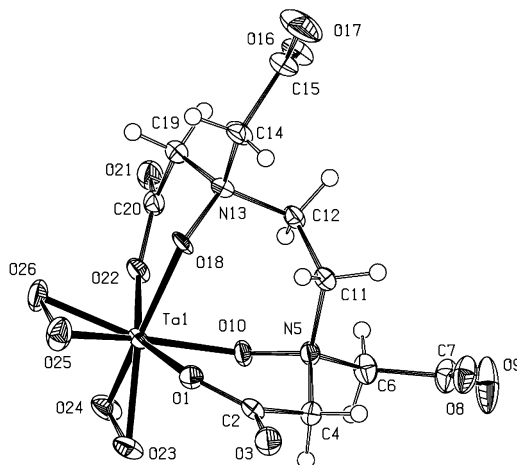


Figure 4. ORTEP plot of the molecular anion $[\text{Ta}(\text{O}_2)_2(\text{edtaO}_2)]^{3-}$ (50% probability).²¹

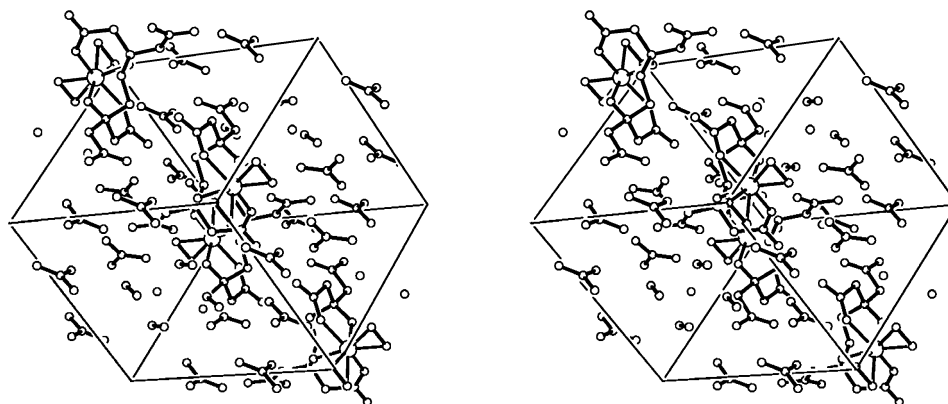


Figure 5. Stereoscopic view of the unit cell of **2b**.

are similar, ranging from 1.961(7) to 2.053(7) Å, and the mean value of the O–O bond length is 1.500(2) Å. The 18 hydrogen atoms of the cations are all involved in at least one hydrogen bond with one of the peroxo groups.

In the crystal structure of complex **2b**, the bis(*N*-oxide) ligand (edtaO₂) is tetradentate and its coordination mode, first deduced from the NMR analysis, is confirmed: two deprotonated carboxylato and two η^1 -*N,O* groups coordinate tantalum. For comparison, the coordination of the *N*–O groups in the niobium and tantalum complexes with hydroxyiminodiacetic acid (hida), [M(hida)₂][−] (M = Nb^V or Ta^V), and 2,2′-(hydroxyimino)dipropionic acid (hidpa), [Nb(hidpa)₂][−], occurs in an η^2 mode¹⁷ just as the similar vanadium derivatives occur, [V^V(hida)₂][−]¹⁸ and [V^V(hidpa)₂][−].¹⁹ Moreover, in complex **2b**, coordination around tantalum is completed by two bidentate peroxo groups. Tantalum exhibits, therefore, an 8-fold coordination as it does in compound **1**. Figure 4 shows the molecular structure of the [Ta(O₂)₂(edtaO₂)]^{3−} anion.

The coordination polyhedron observed in that case is identical to that reported for the niobium derivative, [Nb(O₂)₂(edtaO₂)]^{3−},¹³ and may be described as a triangular dodecahedron, which is rather highly distorted on one side. As indicated in Table 4, in this anion, the four oxygen atoms from the peroxo groups (O23, O24, O25, and O26) are coplanar within experimental error. The maximum deviation from the best mean plane through these four O atoms is less than 0.003 Å. On the opposite side of the polyhedron, the four oxygen atoms from the PAC ligand are not coplanar. In the anions described above, the oxygen atoms from the two carboxylate groups (O1 and O22) and the two *N*-oxide groups (O10 and O18) are observed at quite similar distances from the mean plane of 1.7 and 2.7 Å, respectively (see Table 4).

The mean Ta–O(*N*-oxide) bond distance reaches 2.092(4) Å, a value which is identical to that observed in the niobium complex, (gu)₃[Nb(O₂)₂(edtaO₂)] (2.090(4) Å),¹³ but

- (17) Smith, P. D.; Harben, S. M.; Beddoes, R. L.; Helliwell, M.; Collison, D.; Garner, C. D. *J. Chem. Soc., Dalton Trans.* **1997**, 685–691.
 (18) Carrondo, M. A. A. F.; Duarte, M. T. L. S.; Pessoa, J. C.; Silva, J. A. L.; Dasilva, J. J. R. F.; Vaz, M. C. T. A.; Vilasboas, L. F. *J. Chem. Soc., Chem. Commun.* **1988**, 1158–1160.
 (19) Armstrong, E. M.; Beddoes, R. L.; Calviou, L. J.; Charnock, J. M.; Collison, D.; Ertok, N.; Naismith, J. H.; Garner, C. D. *J. Am. Chem. Soc.* **1993**, *115*, 807–808.

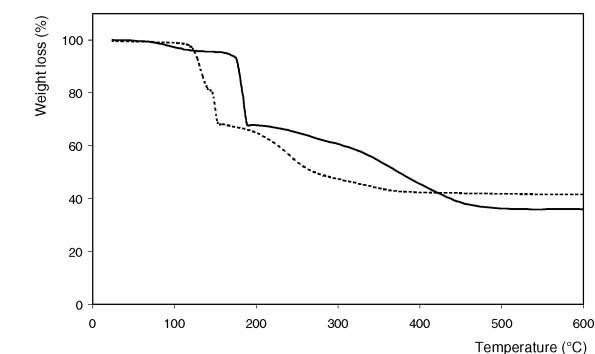


Figure 6. Thermogravimetric analyses of **1** (dashed line) and **2a** (straight line) in air (10 °C/min).

shorter than the mean value displayed by a peroxo-fluoro Ta^V complex with a 2-methylpyridine *N*-oxide ligand, (NET₄)[Ta(O₂)F₄(C₆H₇NO)] (2.20(3) Å).²⁰ The mean value for Ta–O(carboxylato) distances is 2.133(4) Å, which is slightly shorter than in the (gu)₃[Nb(O₂)₂(edtaO₂)] complex (2.152(5) Å). The Ta–O(peroxo) and O–O mean distances are 1.992(4) and 1.494(6) Å, respectively. Moreover, it is worth noting that, for complex **2b**, the mean value of both *N*–O(*N*-oxide) bond lengths is 1.393(6) Å. For comparison, the mean *N*–O distance observed in the crystal structure of the free edtaO₂ ligand is 1.398(2) Å.¹³

For compound **2b**, the cocrystallized water and hydrogen peroxide molecules are involved in an intricate hydrogen-bond network, involving all of the NH₂ groups of the guanidinium counterions, as illustrated by Figure 5.

Thermal Analyses. Compound **1** undergoes a three-step degradation into Ta₂O₅ up to a final decomposition temperature near 370 °C. The thermal behaviors of compounds **2a** and **3** are relatively similar; after dehydration, they undergo a four-step degradation into Ta₂O₅ up to a final decomposition temperature near 470 °C. Because of the presence of peroxo groups, these compounds show a poor thermal stability. Their thermograms display a vigorous exothermal decomposition with a drastic weight loss at 180 and 200 °C, respectively. The thermogravimetric analyses of **1** and **2a** are illustrated in Figure 6.

- (20) Dewan, J. C.; Edwards, A. J. *J. Chem. Soc., Dalton Trans.* **1977**, 981–983.
 (21) Spek, A. L. *PLATON Molecular Geometry Program*; University of Utrecht: Utrecht, The Netherlands, 1998.

Conclusions

New tantalum(V) complexes with peroxo and *N*-oxide derivatives of polyaminocarboxylic ligands have been prepared and characterized from the structural and spectroscopic point of view. Because these compounds exhibit a high solubility in water, they constitute ideal candidates as molecular precursors for Ta-based oxide materials.

Acknowledgment. The authors thank the Belgian National Fund for Scientific Research (FNRS) for the research

fellowship allotted to D.B. and the financial support. They also thank Dr. D. Chapon for carrying out the NMR measurements.

Supporting Information Available: X-ray crystallographic file in CIF format for **1** and **2b**. This material is available free of charge via the Internet at <http://pubs.acs.org>.

IC049639K